A numerical study of the development of bulk scale-free structures upon growth of self-affine aggregates.

Federico Romá[1], Claudio M. Horowitz[2] and Ezequiel V. Albano[2].

1- Departamento de Física, UNSL, Chacabuco 917, (5700), San Luis, Argentina.

2- Instituto de Investigaciones Fisicoquímicas Teóricas y Aplicadas (INIFTA), UNLP, CONICET, Casilla de Correo 16, Sucursal 4, (1900) La Plata, Argentina

Abstract

During the last decade, self-affine geometrical properties of many growing aggregates, originated in a wide variety of processes, have been well characterized. However, little progress has been achieved in the search of a unified description of the underlying dynamics. Extensive numerical evidence has been given showing that the bulk of aggregates formed upon ballistic aggregation and random deposition with surface relaxation processes can be broken down into a set of infinite scale invariant structures called "trees". These two types of aggregates have been selected because it has been established that they belong to different universality classes: those of Kardar-Parisi-Zhang and Edward-Wilkinson, respectively. Exponents describing the spatial and temporal scale invariance of the trees can be related to the classical exponents describing the self-affine nature of the growing interface. Furthermore, those exponents allows us to distinguish either the compact or non-compact nature of the growing trees. Therefore, the measurement of the statistic of the process of growing trees may become a useful experimental technique for the evaluation of the self-affine properties of some aggregates.

PACS numbers: 64.60.Ht, 05.40.+j, 61.43.Hv, 05.70.Ln

I. Introduction.

The study of growth processes has recently attracted considerable attention as a consequence of many factors such as the formulation of the theory of fractals since the pioneering work of Mandelbrot[1], the development of new experimental techniques (e.g. scanning tunneling microscopy) and the availability of computer facilities for graphical and numerical simulations. So far, it is well established that spatial scaling structures originated from growth processes are extremely common in nature. In fact, a great variety of systems exhibit self-affinities over extended ranges of spatial and temporal scales[2–5]. Therefore, extensive theoretical and experimental research has focused on the characterization of the self-affine nature of the structures resulting from growth processes[2–5].

The phenomenological scaling approach to the dynamic evolution of a self-affine interface early developed by Family and Vicsek[6,7] has become a useful tool to characterize self-affine roughness. Considering a flat, $d-1$ dimensional surface at time $t=0$ and pointing the attention to the growing process that occurs essentially parallel to the surface, it is possible to assume without loss of generality that there exists a well defined growth direction and that the interface can be described by a function $h(\mathbf{x},t)$ that gives the height of the interface at time t and position $\mathbf{x}$. Of course, such height is measured from the initial flat surface at t=0. If the interface cannot be described by a single valued function of $\mathbf{x}$, the function $h(\mathbf{x},t)$ gives the maximum height of the interface at $\mathbf{x}$. Considering a section of the sample having a typical size L (in each of the $d-1$ dimensions of the surface) the average height of the interface at time t is defined as:

$$< h(t) >= \frac{1}{(L^{d-1})} \sum_{\mathbf{x}} h(\mathbf{x},t), \tag{1}$$

where the summation runs over all $\mathbf{x}$'s. The interface width $w(L,t)$ at time t may be defined by the rms of the height fluctuations given by:

$$w(L,t) = \left(\left\langle h^2(t) \right\rangle - \left\langle h(t) \right\rangle^2 \right)^{1/2}. \tag{2}$$

The Family-Viscek scaling approach assumes that:

$$w(L,t) = L^{\alpha} F(t/L^{z}), \tag{3}$$

where $F(y) \propto y^{\beta}$ for $y << 1$ and $F(y) \rightarrow constant$ for $y >> 1$, with $z = \alpha/\beta$. Also α, β and z are the roughness, growing and dynamic exponents, respectively.

The dynamic exponent z describes the evolution of a correlated region with time: initially different parts of the interface are independent, but regions of correlated roughness form over time and their size grows as $\xi \propto t^{1/z}$. Thus, for a finite sample of side L and $t \rightarrow \infty$ the width of the growing interface reaches a statistically stationary state so that $w(L) \propto L^{\alpha}$. Furthermore, the overall width of the interface grows as t^{β} until it saturates at L^{α}.

In contrast to the progress achieved in the characterization of the self-affine behavior of interfaces, little attention has been drawn to the description of the internal structure of the growing system. In this work, extensive numerical evidence is presented showing that the bulk of two archetypical growth models, namely ballistic deposition and random deposition with surface relaxation, can effectively be rationalized on the basis of a treeing process; i.e, any growing structure can be thought as the superposition of individual trees. These individual trees can be defined as follows: in the case of the ballistic deposition model (figure 1(a)), a newly deposited particle is assumed to belong to the same tree as that of the nearest neighbor particle where it is attached. If the deposited particle has more than one nearest neighbor belonging to different trees such as particle A in figure 1(a), one of them is selected at random and the particle is incorporated into that tree . In the case of the random deposition with surface relaxation model (figure 1(b)), a newly deposited particle is assumed to belong to the tree corresponding to the impingement site, before its eventual relaxation. See also figure 1 caption for further details.

Those trees that spread out incorporating additional growing centers; e.g. capturing particles, developing new branches, etc., are said to be "alive" (for example trees 1,2 and 4 in figures 1(a) and 1(b)). In contrast, some other trees may stop their growth due to shadowing by surrounding growing trees, so they become "dead trees" such as tree 3 in

figures 1(a) and 1(b). The structure of dead trees is frozen in the sense that it cannot be modified by any further growth. In order to determine the distribution of dead trees one starts the growing process following the specified set of rules and after some fixed time all growing points, i.e. all sites of the aggregate where further growth is still possible, are identified as seeds for these trees. Therefore, the number of such seeds becomes the initial number of trees. During the subsequent process the competition between growing trees dominates the dynamics. Some trees become dead (frozen) and eventually only a single tree may remain.

Within this context, the aim of this work is to perform an extensive numerical investigation of the dynamics of evolving trees of two growing processes, namely Random Deposition with Surface Relaxation (RDSR) and Ballistic Deposition (BD). Furthermore, tests of the scaling relationships relating critical exponents of the treeing process to those describing the self-affine nature of the aggregate are performed in dimensions $1 \leq d \leq 5$. The RDSR and BD processes have been selected because they belong to different universality classes, namely the Edward-Wilkinson (EW)[4,8] and Kardar-Parisi-Zhang (KPZ)[4,9], respectively.

The manuscript is organized as follows: in section II detailed definitions and a discussion of the scaling exponents describing the treeing process and their relationships to exponents related to the self-affine nature of the aggregate are reviewed. In section III a brief description of both the RDSR and BD models and the numerical simulation technique is provided. The results are presented and discussed in section IV while the conclusions are stated in section V.

II. Treeing and self-affinity. Scaling relationships.

Let us consider an aggregate that is growing above a d-dimensional substrate. Such aggregate is formed by trees that compete with each other leading to the entire pattern. The structural properties of both the trees and the resulting entire aggregate are determined by the growth mechanism. In these context, Racz and Vicsek[10] have shown that for self-similar

fractals the tree size distribution that results from the competitive growth process is related to the structure of both the entire aggregate and the individual trees. Subsequently, this concept was extended to the case of self-affine objects[11].

In the following paragraphs we will briefly outline the well known[10,11] relevant definitions and the scaling relationship in order to establish the framework for the subsequent numerical study. Pointing our attention to dead trees of size s (s is the number of particles belonging to the tree) one has that both the rms height (h_s) and the rms width (w_s) of the trees obey simple power laws given by

$$h_s \propto s^{\nu_\parallel}, \tag{4}$$

and

$$w_s \propto s^{\nu_\perp}, \tag{5}$$

where $\nu_\parallel$ and $\nu_\perp$ are the correlation length exponents parallel and perpendicular to the growing direction of the aggregate[11]. These exponents may be different for self-affine (anisotropic) aggregates, while for self-similar objects $\nu_\parallel$=$\nu_\perp$.

Assuming that N_T is the total number of particles of the aggregate, the average particle number N per unit area of the substrate is given by

$$N = N_T/L^d, \tag{6}$$

where particles grow on a d-dimensional hypercubic substrate of size L in a D-dimensional space.

Defining the number of trees with s particles $N_s(N)$ in the whole aggregate one has that

$$N_T = \sum_s s N_s(N), \tag{7}$$

and the cluster size distribution $\mathrm{n}_s(\mathrm{N})$ that gives the probability of having trees of size s per unit area of the substrate is given by

$$n_s(N) = N_s(N)/L^d. \tag{8}$$

Replacing Eqs. (6) and (8) in (7) gives[10,11]

$$N = \sum_s s n_s(N). \tag{9}$$

During the competition between trees along the evolution of the aggregate it may occur that the existence of large neighboring trees may inhibit the growing of smaller ones. This competing process ultimately leads to the death of some trees that become "frozen" within the underlying aggregate. These prevailing large trees continue the competition within more distant trees in a dynamic process. Since this situation takes place on all scales, it is reasonable to expect that the cluster size distribution should exhibit a power-law behavior so that

$$n_s(N) \sim s^{-\tau} f(s^\sigma/N), \tag{10}$$

where τ is an exponent and $f(y)$ is a scaling (cut off) function so that their asymptotic behavior is given by $f(y) \approx 1$ for $y \ll 1$ and $f(y) \approx 0$ for $y \gg 1$.

Substituting (10) in (9) and after some algebra one can obtain[10]

$$\sigma = 2 - \tau. \tag{11}$$

Furthermore, recalling that the competition among trees actually is a dynamic process evolving in time ($t \propto N_t$), one has that the survival time distribution of the trees (n_t) may also obey a simple power-law behavior given by

$$n_t \propto t^{-\gamma}, \tag{12}$$

where γ is an exponent. Therefore, one can establish a relationship between the size and the survival time t of the dead trees so that

$$s \sim t^{1/x}, \tag{13}$$

where the exponent x is given by

$$x = (\tau - 1)/(\gamma - 1). \tag{14}$$

Also, it is reasonable to expect that for the trees $h_s \propto t$, so inserting this relation in equation (13) and comparing it with equation (4) gives

$$x = \nu_{\|}. \tag{15}$$

Let us now establish a relationship between the growing trees and the properties of the aggregate. Assuming that the aggregate is self-similar (even compact) with fractal dimension D, its rms height h is expected to scale as

$$h \sim N^{\nu_l}, \tag{16}$$

for $h << L$, where ν_l is an exponent[11].

However, for length scales $>> h$ the aggregate is uniform in the remaining d lateral directions. This fact, in connection to equations (6) and (16) gives[11]

$$D = \nu_l^{-1} + d. \tag{17}$$

The rms height h of the aggregate can be rewritten as

$$h^2 = \frac{1}{N_T}\sum_i h_i^2 = \frac{1}{NL^d}\sum_s (\sum_{i\in s} h_i^2) N_s(N), \tag{18}$$

where h_i is the distance of the i-th particle from the substrate. Taking into account that the average rms height of a tree of size s is given by

$$h_s^2 = \frac{1}{s}\sum_{i\in s} h_i^2, \tag{19}$$

equation (18) can be rewritten as

$$h^2 = \frac{1}{N}\sum_s s h_s^2 n_s(N), \tag{20}$$

where equation (8) has been used.

Replacing equations (4),(10) and (16) in (20) and performing some algebra one obtains the scaling relationship[11]

$$2\nu_l = -1 + (2 + 2\nu_{\|} - \tau)/\sigma. \tag{21}$$

Now, using equation (11) and (17) it follows that

$$\sigma = \nu_{\parallel}/\nu_l = \nu_{\parallel}(D-d), \tag{22}$$

and substituting equation (22) in equation (11) one has[11]

$$\tau = 2 - \nu_{\parallel}(D-d). \tag{23}$$

The scaling relationship (23) links the exponent τ related to the tree size distribution to the correlation length exponent of the aggregate $\nu_{\parallel}$. It is interesting to notice that $\nu_{\perp}$ is absent in equation (23) due to the fact that during the competitive growth process larger trees prevent smaller ones from growing. Scale invariance in the size distribution of the trees (equation(10)) is a result of this competitive process that is mainly governed by the tree hight (equation(4)).

A typical example for the application of equation (23) is the growth of compact aggregates where $D = d + 1$. So, equation (23) becomes

$$\tau = 2 - \nu_{\parallel}. \tag{24}$$

Also, using equations (14), (15) and (23) one obtains

$$\gamma = 1/\nu_{\parallel}. \tag{25}$$

There is no reason to expect that a compact aggregate may result from the addition of compact trees. In fact, the volume of trees of size s (v_s) scales as

$$v_s \sim h_s w_s^{D-1} \sim s^{\nu_{\parallel}+(D-1)\nu_{\perp}}, \tag{26}$$

and we define the following relationship between the volume and the number of particles $v \sim s^{\pi}$, where π is an exponent, so one has

$$\nu_{\parallel} + (D-1)\nu_{\perp} = \pi, \tag{27}$$

where for compact trees one has $\pi = 1$ while for non-compact trees one has $\pi > 1$.

Identifying the parallel correlation length with $w(s)$ and the time with $h(s)$, one has[13]

$$z = \nu_{\parallel}/\nu_{\perp}. \tag{28}$$

Using equations (14), (15), (23), (27) and (28) for trees in a compact aggregate ($D = d + 1$), we can obtain the following relationships

$$\nu_{\parallel} = \pi z/(z + D - 1), \tag{29}$$

$$\nu_{\perp} = \pi/(z + D - 1), \tag{30}$$

$$\tau = ((2 - \pi)z + 2(D - 1))/(z + D - 1), \tag{31}$$

and

$$\gamma = (z + D - 1)/(\pi z) \tag{32}$$

All these relationships establish links among exponents that characterize the self-affine nature of the interface of the aggregate ($z = \alpha/\beta$) and those corresponding to the description of the treeing process occurring in the bulk ($\nu_{\parallel}$,$\nu_{\perp}$,τ,γ,π).

III. The RDSR and BD models. Simulation methods and mesoscopic equations.

In the random deposition with surface relaxation (RDSR) model a particle is released from a random position above the surface and falls vertically until it reaches the top of the selected column. Of course, such particle is initially located at a distance larger than the maximum height of the interface. The deposited particle is allowed to relax to a nearest neighbor column if the height of the neighboring column is lower than the one corresponding to the selected column. Further details on RDSR aggregates can be found in references[4,8]. Concerning the dynamics of tree formation, it is worth remembering the procedure used to

define a tree. In the case of the RDSR model, a newly deposited particle is assumed to belong to the tree corresponding to the impingement site, before its eventual relaxation.

The ballistic deposition (BD) model is rather simple to describe: a particle is released from a random position above the interface of length L. Subsequently, the particle follows a straight vertical trajectory until it reaches the interface, whereupon it sticks. In contrast to the RDSR model, in the BD model no further relaxation of the particle is considered. Snapshot configurations of BD aggregates, and further details on the deposition rules can be found in references[4,9]. Let us also remember that, in this case, trees are formed assuming that any newly deposited particle belongs to the same tree as that of the nearest neighbor particle where it is attached. If the deposited particle has more than one nearest neighbor belonging to different trees, one of them is selected at random and the particle is incorporated into that tree.

RDSR and BD aggregates are grown in the direction perpendicular to d-dimensional substrate, i.e. in $(d+1)$-dimensions, using samples of different sizes (L^d) with $1 \leq d \leq 5$. Simulation results are averaged over many different runs, depending on L and d. A Monte Carlo time step (mcs) involves the deposition of L^d particles.

The interface of these aggregates is defined as the set of particles that are placed at the highest position of each column. So, the mean height of the interface (equation(1)) and the interface width (equation(2)) can be calculated and both are measured in lattice units (LU). It is well known that these aggregates are self-affine and the width of the growing interface $w(L,t)$ scales as equation (3)[4].

In contrast to the microscopic details of the growing mechanisms of the interface in both models, continuous equations focus on the macroscopic aspects of the roughness. Essentially, the aim is to follow the evolution of the coarse-grained height function $h(x,t)$ using a well-established phenomenological approach that takes into account all the relevant processes that survive at a coarse-grained level.

This procedure normally leads to stochastic nonlinear partial differential equations that may be written as follows[4,8,9,12,14,15]

$$\frac{\partial h(\mathbf{x},t)}{\partial t} = G_i\{h(\mathbf{x},t)\} + F + \eta(\mathbf{x},t), \tag{33}$$

where the index i symbolically denotes different processes, $G_i\{h(\mathbf{x},t)\}$ is a local functional that contains the various surface relaxation phenomena and only depends on the spatial derivatives of $h(\mathbf{x},t)$ since the growth process is determined by the local properties of the surface. Also, F denotes the mean deposition rate and $\eta(\mathbf{x},t)$ is the deposition noise that determines the fluctuations of the incoming flux around its mean value F. It is usually assumed that the noise is spatially and temporally uncorrelated, so fluctuations are given by a Gaussian white noise

$$\langle \eta(\mathbf{x},t) \rangle = 0, \tag{34}$$

and

$$\langle \eta(\mathbf{x},t)\eta(\mathbf{x}`,t`) \rangle = 2C\delta^d(\mathbf{x}-\mathbf{x}`)\delta(t-t`), \tag{35}$$

where the brackets denote ensemble averaging, C is the strength of the fluctuations, and d the spatial dimension of the surface.

The RDSR model can be described by the Edwards-Wilkinson equation given by[4,8,12,16]

$$\frac{\partial h(\mathbf{x},t)}{\partial t} = F + \nu_o \nabla^2 h(\mathbf{x},t) + \eta(\mathbf{x},t), \tag{36}$$

where ν_o plays the role of an effective surface tension, since the $\nu_o \nabla^2 h(\mathbf{x},t)$ term tends to smooth the interface. Equation (36) can be solved in Fourier space and the following values of the exponents are obtained: $z = 2$, $\alpha = (2-d)/2$ and $\beta = (2-d)/4$. So, there exists an upper critical dimension $d_c = 2$ above which one has $\alpha = 0$ and $\beta = 0$.

The BD model can be described by the Kardar-Parisi-Zhang equation given by[9]

$$\frac{\partial h(\mathbf{x},t)}{\partial t} = F + \nu \nabla^2 h + \frac{\lambda}{2}(\nabla h)^2 + \eta(\mathbf{x},t), \tag{37}$$

where λ plays the role of an effective lateral growth. In this equation, the exponents satisfy the scaling relation

$$z + \alpha = 2, \tag{38}$$

as a consequence of Galilean invariance in the related Burgers equation[17]. In the usual field theory approach, a perturbation theory is defined with respect to the nonlinear term (λ). The corresponding renormalization group reveals[18] that the physics of the KPZ is related to a strong coupling fixed point, which is inaccessible by perturbative methods. Except for $d = 1$, where, thanks to a fluctuation-dissipation theorem, an analytic solution is possible. In this case one has $\alpha = 1/2$, $\beta = 1/3$, so that $z = 3/2$. Extensive numerical simulations have been carried out for restricted solid on solid models[19]. These are discrete models that belong to the KPZ universality class[20] and these studies show a gradual decrease in the value of α, without any evidence for an upper critical dimension. In the same direction a recent study performed using a nonperturbative renormalization of the KPZ equation suggests a gradual decrease in the value of α[21]. On the other hand, several analytical approaches[22] suggest an upper critical dimension $d_c = 4$ above which one should have $\alpha = 0$.

IV. Results and discussion.

Figure 2 shows the tree distribution functions corresponding to the RDRS model in dimension $1 \leq d \leq 5$. The tree size distribution (figure 2 (a)) for $d = 1$ exhibits a power law according to Eq.(10) with exponent $\tau = 1.35 \pm 0.03$. For higher dimensions n_s also exhibits power law behavior but the slope $\tau = 1.50 \pm 0.01$ becomes independent of the dimensionality. A similar behavior is shown by the survival time distribution (figure 2(b)) that has slopes $\gamma = 1.54 \pm 0.03$ for $d = 1$ and $\gamma = 2.00 \pm 0.03$ for $d \geq 2$, respectively. The measured exponents are listed in Table I.

The distribution functions of the BD model also exhibit power law behavior (figure (3)). However, in contrast to the case of RDSR, for both n_s (figure 3(a)) and n_t (figure 3(b)) the slopes depend on the dimensionality. The measured exponents are listed in the 5^{th} and 9^{th} columns of Table II.

The behavior of the rms height of the trees as a function of the tree size s is shown in figures 4(a) and 4(b) for RDSR and BD, respectively. Again, nice power laws are observed in all cases. For the RDSR model a clear change in the slope is observed between $d = 1$ and $d \geq 2$, where for the higher dimensions the slopes are independent of the dimensionality (see 3^{rd} column of Table I). For the BD model the slopes are different in all dimensions (see 3^{rd} column of Table II).

Results shown in figure 5 for the rms width of the trees (w_s) versus s are also fully consistent with the previous results and are listed in the 2^{nd} column of Tables I and II.

Based on our numerical estimation of the exponents τ, γ, $\nu_\perp$ and $\nu_\parallel$ we are in a condition to check the scaling relationships discussed in section II that are summarized by equations (24), (27), (28), (31), (32) and (38), where the latter only holds for the BD model.

The results obtained for the RDSR model (Table I) show that the exponents $\nu_\perp$, $\nu_\parallel$, τ and γ are independent of the dimensionality of the surface for $d \geq 2$, as expected from figures 1-4. These results are consistent with the fact that $d = 2$ is the upper critical dimension of the EW universality class.

Inserting the exact value $z = 2$ for the EW universality class in equation (31) the "theoretical" estimation of τ can be obtained (7^{th} column of Table I), which is in excellent agreement with the numerical data. Also, inserting the measured values of $\nu_\parallel$ in equation (24) (see the 6^{th} column of Table I) excellent agreement with the measured exponents is obtained. The quality of the achieved agreement is also excellent when comparing theoretical and estimated (equation (25)) values of γ, which is shown in the 10^{th} and 9^{th} columns of Table I, respectively.

For the case of the RDSR model it is interesting to notice that the exponent π (4^{th} column of Table I) departs from the trend exhibited by the other exponents. In fact, while $\pi \sim 1$ for $d \leq 2$, such an exponent increases monotonically with the dimensionality for $d > 2$. Roughly, an average increment of $1/4$ in π for each additional dimension is estimated. The value of $\pi = 1$ corresponds to the development of compact trees (see equations (26),(27)), so it is concluded that for $d > 2$ the trees leading to the formation of RDSR aggregates

are non-compact objects. Therefore, the branches of the trees become interweaved forming complex patterns.

Our results for the BD model are listed in Table II. In this case the measured exponents ($\nu_\perp$, $\nu_\parallel$, τ and γ) depend on the dimensionality, as expected from figures $2-5$. The measured values of τ (5^{th} column of Table II) are in agreement with the estimation obtained using equation (24) (6^{th} column of Table II) for $d \leq 4$. For $d = 5$ this estimation presents a small deviation due to the large error involved in the evaluation of the exponent. However, a slight increment of τ with the dimensionality is found in both cases (the measured exponent and equation (24)). This result is in contrast to the conjecture stating that $d = 4$ may be the upper critical dimension of the KPZ universality class[19]. Furthermore, using equations (31), (38) and the values of α reported in reference [25] two additional comparisons can be made: inserting the values of z obtained using renormalization group calculations (numerical simulation) in equation (31) gives the values of τ listed in the 7^{th} (8^{th}) column of Table II. In both cases, excellent agreement with the measured exponents is found.

We have to recognize large errors in our evaluation of γ for the BD model (see figure 2(b)) that prevent reliable estimations for $d \geq 4$. However, comparisons with results obtained using equation (25) (10^{th}column of Table II), renormalization group calculation (11^{th} column of Table II) and numerical evaluation (12^{th} column of Table II), exhibit the trend already observed by our direct measurement of γ.

It should also be noticed that $\pi \sim 1$ (within error bars) pointing out that BD aggregates are built up by compact trees at least for $d \leq 4$, in contrast with our previous results obtained for RDSR aggregates for $d > 2$.

CONCLUSIONS.

Extensive numerical evidence is provided showing that the bulk of two typical growth models, belonging to both the KPZ and EW universality classes, can be rationalized in terms of a treeing process. Scaling relationships, linking exponents relevant to the treeing

process with standard dynamic exponents are reviewed and tested numerically in dimensions $1 \leq d \leq 5$. So, our main conclusions are summarized in Tables I and II where all the measured exponents are listed and compared to theoretical predictions. It is concluded that BD trees are compact objects (at least up to $d = 4$) while RDSR trees are non-compact objects for $d > 2$ leading to interweaved complex structures. Based on the validity of equations (29-32) and since above the upper critical dimension the exponents $\nu_{\parallel}$, $\nu_{\perp}$, τ, and γ remain constant for self-similar aggregates, it can be stated that above the upper critical dimension the change in the dimensionality of the aggregate implies that π must also change. Therefore, we conjectured that all kinds of self-affine aggregates above their upper critical dimension can be rationalized in term of the superposition of non-compact trees.

Summing up, it is shown that the evolution of the treeing statistics is a suitable method for the characterization of the growing aggregates with promising applications in experimental situations. In fact, it is well known that the electrochemical deposition method in thin cells provides a rather simple experimental setup for the observation of a wide variety of self-affine growing patterns[23,24]. In this case the dynamics of growing trees leading to frozen structures can easily be observed and the evaluation of the tree size distribution can be obtained straightforwardly after proper digitalization of the images of the aggregates. Another field of application is the study of polycrystalline thin film growth by scanning tunneling microscopy[25,26] and atomic force microscopy[27]. In these cases the direct evaluation of the number of crystallites as a function of the deposit height accounts for the number of frozen crystallites (i.e. the trees of the growing aggregate) and the crystallite size distribution can be evaluated.

ACKNOWLEDGMENTS. This work was financially supported by CONICET, UNLP and ANPCyT (Argentina).

Table I: List of exponents $\nu_\perp$, $\nu_\parallel$, τ (5^{th} column) and γ (8^{th} column) measured for the RDSR model for dimensions $1 \leq d \leq 5$. The values of theoretical estimations of τ and γ are obtained taking $z = 2$ in Equation (31) (7^{th} column) and Equation (32) (10^{th} column), respectively. For these estimations $\pi = 1$ for $d \leq 2$ and $\pi = 5/4,\ 3/2,\ 7/4$ for $d = 3, 4, 5$, have been used, respectively. The values of π obtained using Equation (27) are shown in the 4^{th} column. The values of τ and γ obtained using Equations (24) and (25) are shown in the 6^{th} and 9^{th} columns, respectively.

D	$\nu_\perp$	$\nu_\parallel$	π	τ	τ(Eq.24)	τ(t)	γ	γ(Eq.25)	γ(t)
1+1	0.35(2)	0.63(1)	0.98(2)	1.35(3)	1.37(1)	4/3	1.54(3)	1.59(3)	3/2
2+1	0.27(2)	0.50(1)	1.02(4)	1.49(1)	1.50(1)	3/2	1.98(5)	2.00(4)	2
3+1	0.26(2)	0.50(1)	1.28(6)	1.50(3)	1.50(1)	3/2	2.00(2)	2.00(4)	2
4+1	0.25(2)	0.50(1)	1.50(8)	1.50(1)	1.50(1)	3/2	1.99(2)	2.00(4)	2
5+1	0.25(1)	0.49(1)	1.74(4)	1.50(2)	1.51(1)	3/2	1.99(4)	2.04(4)	2

Table II: List of exponents $\nu_\perp$, $\nu_\parallel$, τ (5^{th} column) and γ (9^{th} column) measured for the BD model for dimensions $1 \leq d \leq 5$. The estimations performed using Equations (24) and (25) are shown in the 6^{th} and 10^{th} columns, respectively. The exponents obtained using Equations (31), (32) and (38), $\pi = 1$ and α values obtained by renormalization group calculation (RG) and numerical simulations (NS) reported in reference[21] are shown in the 7^{th}, 8^{th}, 11^{th}, 12^{th} columns. The exponent π is evaluated using equation (27) (4^{th} column).

D	$\nu_\perp$	$\nu_\parallel$	π	τ	τ(Eq.24)	τ(RG)	τ(NS)	γ	γ(Eq.25)	γ(RG)	γ(NS)
1+1	0.40(1)	0.60(1)	1.00(2)	1.40(1)	1.40(1)	1.40	1.40	1.70(2)	1.66(3)	1.66	1.66
2+1	0.29(1)	0.45(1)	1.03(2)	1.57(1)	1.55(1)	1.54	1.55	2.3(1)	2.22(5)	2.22	2.24
3+1	0.23(2)	0.38(1)	1.07(6)	1.65(1)	1.62(1)	1.63	1.64	3.2(2)	2.63(7)	2.75	2.77
4+1	0.21(4)	0.34(2)	1.18(16)	1.70(2)	1.66(2)	1.69	1.70	-	2.94(15)	3.27	3.30
5+1	-	0.33(4)	-	1.75(3)	1.67(4)	1.73	1.73	-	3.0(3)	3.78	3.76

REFERENCES

[1] B. Mandelbrot, in "The Fractal Geometry of Nature", Freeman, San Francisco, 1982.

[2] A. Bunde and S. Havlin (eds.), in "Fractals and Disordered Sytems", Springer Verlag, Berlin, 1991.

[3] J. Feders, in "Fractals", Plenum Press, New York, (1988).

[4] A. L. Barabasi and H. E. Stanley, in "Fractal Concepts in Surface Growth." Cambridge University Press, Cambridge (1995).

[5] J. Kertész and T. Vicsek, Self-Affine Interfaces, in Fractals in Science, Edited by A. Bunde and S. Havlin. Springer-Verlag, Berlin (1995), Page 89.

[6] F. Family, Rough surfaces: Scaling Theory and Universality, edited by R. Jullien, L. Peliti, R. Rammal, and N. Boccara, Springer Proceedings in Physics Vol.32 (Springer-Verlag, Berlin, 1988), p.193.

[7] F. Family, T. Vicsek, J. Phys. A., **18**, L75 (1985).

[8] S. F. Edwards and D. R. Wilkinson, Proc. Roy. Soc. London A **381**, 17 (1982).

[9] M. Kardar, G. Parisi and Y. -C. Zhang, Phys. Rev. Lett. **56**, 889 (1986).

[10] Zoltán Rácz and Tamás Vicsek, Phys. Rev. Lett. **51**, 2382 (1983).

[11] M. Matsushita and P. Meakin, Phys. Rev. A **37**, 3645 (1988).

[12] M. Kardar. Physica A, **281**, 295 (2000).

[13] J. Krug and P. Meakin, Phys. Rev. A **40**, 2064 (1989).

[14] M. Kardar, in J. C. Charmet, S. Roux, E. Guyon (Eds.), Disorder and Fracture, Plenum, New York, page 3, (1990).

[15] M. Kardar and J. Turkish, J. Phys. **18**, 221 (1994).

[16] Thomas Nattermann and Lei-Han Tang, Phys. Rev. A **45**, 7156 (1992).

[17] D. Foster, D. R. Nelson, and M. J. Stephen, Phys. Rev. A **16**, 732 (1977).

[18] T. Halpin-Healy and Y. C-. Zhang, Phys. Rep. **254**, 215 (1995).

[19] T. Ala-Nissila et al., J. Stat. Phys. **72**, 207 (1993); L. -H. Tang et al., Phys. Rev. A **45**, 7162 (1992).

[20] M. Marsili, A. Maritan, F. Toigo, and J. R. Banavar, Rev. Mod. Phys. **68**, 963 (1996).

[21] C. Castellano, M. Marsili, and L. Pietronero. Phys. Rev. Lett. **80**, 3527 (1998).

[22] T. Halpin-Healy, Phys. Rev. A **42**, 711 (1990); M. A. Moore et al., Phys. Rev. Lett. **74**, 4257 (1995); J-P. Bouchaud and M. E. Cates, Phys. Rev. E **47**, 1455 (1993).

[23] J. Elezgaray, C. Léger and F. Argoul, Phys. Rev. Lett. **84**, 3129 (2000).

[24] P. Schilardi, O. Azzaroni, R. Salvarezza and A. Arvia, Phys. Rev. B, **59**, 4638 (1999).

[25] E. Albano, R. Salvarezza, L. Vázquez, and A. Arvia. Phys. Rev. B. **59**, 7354 (1999).

[26] L. Vázquez, R. Salvarezza, E. Albano, A. Arvia, A. Hernádez Creus, R. Levy and J. Albella. Adv. Mat. **4**, 89 (1998).

[27] F. Ojeda, R. Cuerno, R. Salvarezza and L. Vázquez, Phys. Rev. Lett. **84**, 3125 (2000).

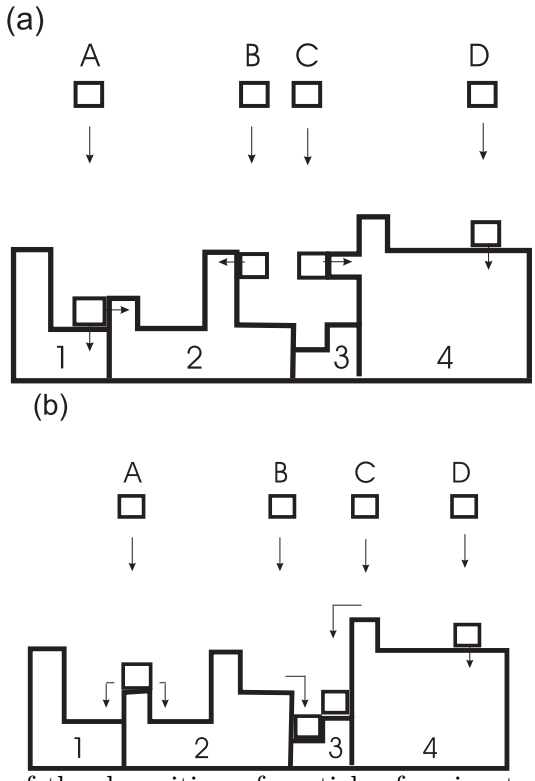

FIG. 1. Schematic view of the deposition of particles forming trees. In (a) the particles are deposited with the rules of ballistic deposition. Particle A belongs to tree 1 or 2 with the same probability, particle B belongs to tree 2 and particles C and D belong to tree 4. The growth of tree 3 is stopped after particle C deposition and it becomes a frozen tree. In (b) the particles are deposited with the rules of random deposition with surface relaxation. Particle A, which belongs to tree 2, can either relax to the right or to the left with the same probability. Notice that in the former, particle A partially shadows tree 1, while in the latter it simply becomes attached to tree 2. Particle B belongs to tree 2 but it relaxes on top of tree 3 causing partial shadowing. Particle C belongs to tree 4 and after relaxation on top of tree 3 causes the growth of that tree to stop, so that it becomes a frozen tree. Finally, particle D belongs to tree 4.

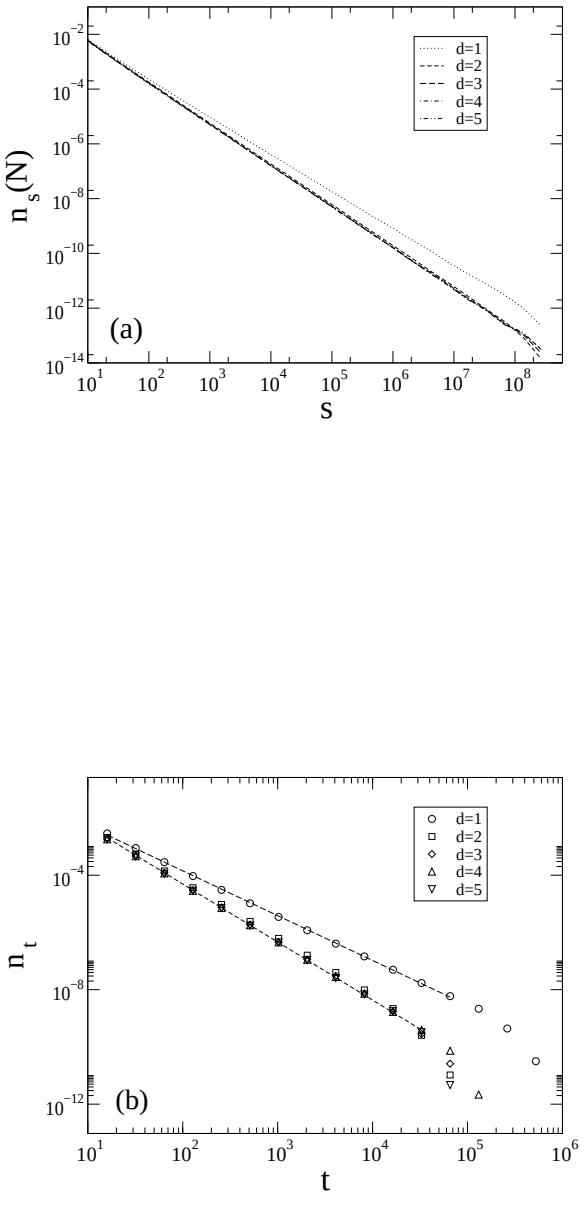

FIG. 2. Log-log plots of the tree distribution functions corresponding to the RDRS model in dimensions $1 \leq d \leq 5$. (a) The tree size distribution, where the size s is given by the number of particles of each tree. (b) The survival time distribution, where the time is measured in mcs.

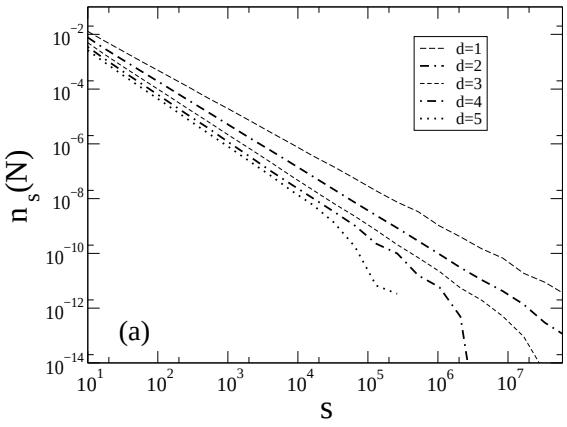

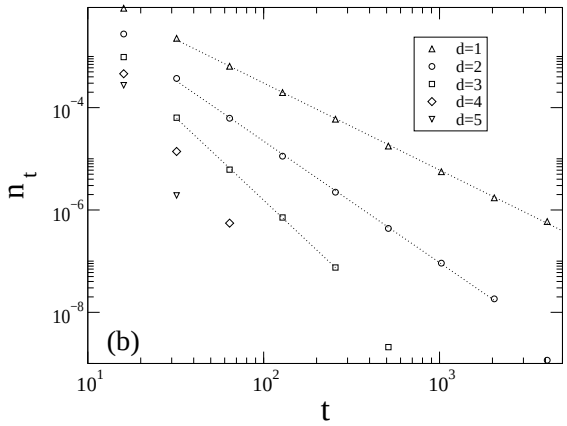

FIG. 3. Log-log plots of the tree distribution functions corresponding to the BD model in dimensions $1 \leq d \leq 5$. (a) The tree size distribution where the size s is given by the number of particles of each tree. (b) The survival time distribution, where the time is measured in mcs.

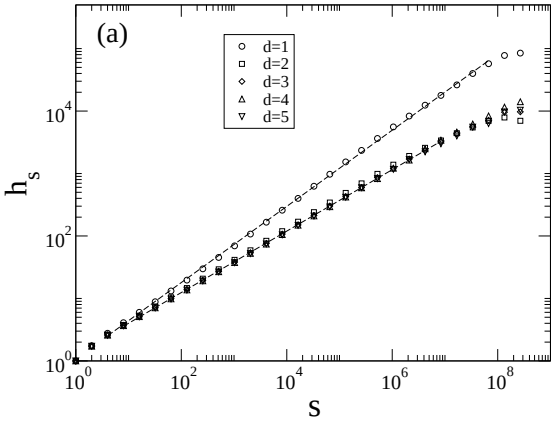

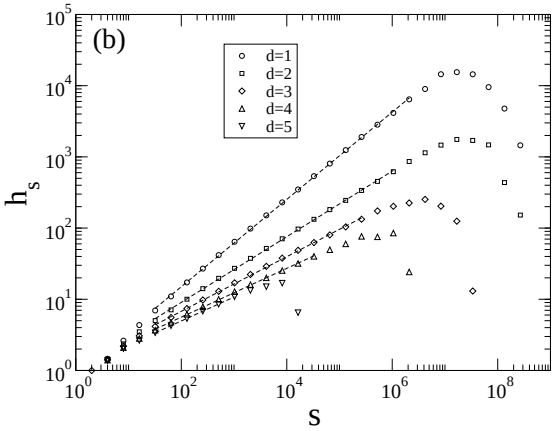

FIG. 4. (a) and (b) Log-log plots of rms height of the trees as a function of the tree size s for the RDSR model and the BD model, respectively. The rms height is measured in LU and the size s is given by the number of particles of each tree.

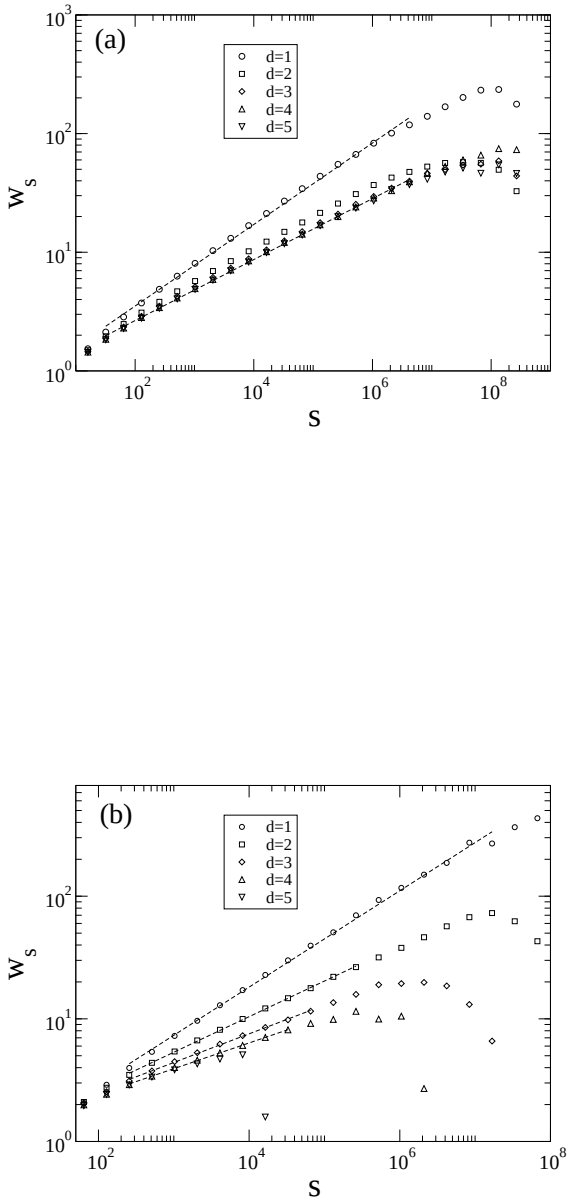

FIG. 5. (a) Log-log plots of rms width of the trees as a function of the tree size s for the RDSR model. (b) Log-log plots of rms width of the trees as a function of the tree size s for the BD model. The rms width is measured in LU and the size s is given by the number of particles of each tree.